PILOTED SIMULATION ASSESSMENT OF MINIMUM-ENERGY TRANSITION CONTROL STRATEGIES

Namuk Kang, Linghai Lu, James Whidborne, Declan Saunders and Wen-Chin Li
Cranfield University, Cranfield, United Kingdom

Abstract

This paper presents a piloted simulation study aimed at assessing the practicality and usability of minimum-energy conversion and reconversion trajectories and flight control system for vectored-thrust eVTOL aircraft when flown by flight-naïve operators. The investigation evaluates whether such energy-optimal profiles can be feasibly and effectively tracked using manual control, both with and without visual target command guidance. Objective performance measures based on Flight Test Manoeuvre (FTM) criteria and eye-tracking metrics, combined with subjective assessments of NASA Task Load Index and specifically designed comfort ratings, were employed to quantify task performance and cognitive workload. The results demonstrate that minimum energy transitions are generally flyable by up to untrained users, particularly when aided by the proposed target command guidance system, which yielded a 92% compliance rate with the FTM desired criteria (Level 1) handling qualities (HQ) across participant groups. The study further identifies that cognitive workload and HQ were influenced by control sensitivity variations during conversion, and by the prolonged tracking of incrementally changing target commands during reconversion. In response, design recommendations are proposed to enhance pilot usability with potential trade-offs in the fundamental energy efficiency objectives. These findings contribute to the ongoing development of pilot-autonomy interaction strategies and transition guidance systems for next-generation AAM vehicles.

1. INTRODUCTION

The emergence of eVTOL aircraft signifies a transformative shift in the evolution of the AAM aviation sector [1]. Within the eVTOL design space, vectored-thrust and LPC configurations have gained prominence due to their superior cruise efficiency and extended operational range compared with multicopter architectures [2]. These performance advantages are especially important given the present limitations in battery energy density and power capacity, which restrict mission endurance and payload capabilities of electric propulsion systems [3]. However, the adoption of compound eVTOL configurations introduces the need for a transition phase between hover and forward flight-encompassing both conversion and reconversion manoeuvres, which entails unique control challenges not encountered in single-regime aircraft. These flight phases require complicated control challenges that diverge from those observed in single-mode aircraft operations. While prior research has addressed the dynamic characteristics and control law requirements during these transitions [4-5], the derivation of energy-optimal transition strategies remains highly dependent on vehicle-specific parameters and design constraints.

Several recent studies have explored energy-optimal trajectories and power-efficient transition profiles for various tilt-wing and tiltrotor eVTOL configurations [6-9]. These approaches commonly employ optimisation techniques to minimise energy consumption during mode transitions while satisfying flight envelope constraints. Nevertheless, whether such optimal transition profiles are tractable and flyable by human operators, particularly by flight-naïve individuals not yet been thoroughly evaluated. The practical realisation of energy-optimal performance in piloted scenarios remains an open question.

From an operational standpoint, human-in-the-loop control will remain essential in the near term, because full-scale autonomous eVTOL deployment is unlikely before 2035 due to regulatory challenges [10]. Consequently, research into Pilot-Automation Interaction (PAI) is of growing importance to characterise the spectrum of pilot-autonomy relationships under varying levels of automation [11]. This study situates itself within a PAI-1 to PAI-2 boundary, where the pilot is responsible for manually tracking command cues with limited augmentation. The current study operates within a regime below PAI-2, where pilots are responsible for manually tracking target command guidance with only intermittent assistance from automated control modes. However, the behavioural dynamics between pilot responses and system-provided guidance cues under energy constraints, particularly for flight-naïve participants, remain insufficiently investigated.

Existing work from the EU MyCopter project [12-13] identified Acceleration Command Speed Hold (ACSH) as a preferable control response mode for flight-naïve operators, especially in personal aerial vehicle (PAV) and transition flight contexts, offering favourable HQ ratings. This response type is increasingly prevalent in eVTOL control architectures [11], though ergonomic and cognitive challenges may persist. Although fixed-base simulations have demonstrated acceptable performance in precision control and low-speed flight tasks using ACSH response types [14], the response was not less intuitive for the professional test pilots. The research test pilots required more practice to achieve proficiency, particularly when compared with conventional attitude rate control system. Response type has also been shown to influence pilot delay and compensation behaviour [15], reinforcing the importance of evaluating cognitive workload and attentional demand in ACSH-based systems. To mitigate these challenges, prior work has explored optic flow and tau-based guidance to support landing tasks for flight-naïve pilots under ACSH response conditions [16]. Even though comprehending a pilot's cognitive workload is fundamental to the piloted flight simulation [17], no study has yet quantitatively examined visual attention or cognitive workload, particularly during the conversion and reconversion of vectored-trust aircraft operating under minimum energy conditions.

To address these research gaps, the present study investigates whether flight-naïve participants can successfully execute minimum-energy conversion and reconversion manoeuvres using guidance-based control. Performance is assessed through both objective metrics, including FTM-based evaluation criteria and gaze-derived attention measures, and subjective metrics such as NASA TLX workload ratings [18] and a specially designed five-item comfort scale developed with the assistance of the Human Factors team at Cranfield.

The remainder of this paper is organised as follows. First, the experimental setup and simulation environment used to capture pilot trajectory performance are presented. The subsequent section presents the piloted evaluation results under both guidance-assisted and unguided conditions. This is followed by a discussion of the implications for flight-naïve pilot usability and eVTOL system design. Finally, the paper concludes with a summary of key findings and implications for future research.

2. AIRCRAFT MODELLING DESCRIPTION

2.1. Aston Martin Volante Vision

The Aston Martin Volante Vision Concept model, illustrated in Figure 1, is adopted as the research aircraft in this thesis. This concept design was developed in collaboration with Cranfield Aerospace Solutions, Cranfield University, and Rolls-Royce. Its configuration parameters and performance metrics are summarised in Table 1.

Figure 1 Aston Martin Volante Vision concept.

Table 1 Volante Vision aircraft configuration parameters.

Characteristic	Imperial	Metric
Max gross weight	3,306 lb	1,500 kg
Roll inertia, I_{xx}	1,230 slug ft2	1,668 kg m2
Pitch inertia, I_{yy}	4,484 slug ft2	6,079 kg m2
Yaw inertia, I_{zz}	5,700 slug ft2	7,728 kg m2
Product inertia, I_{xz}	−125 slug ft2	−169 kg m2
Passengers	2 to 3 pax + 1 crew	
Wingspan	28.0 ft	8.5 m
Length	31.0 ft	9.6 m
Height	5.6 ft	1.7 m
Range	162 nm	300 km
Service ceiling	3,000 ft	914 m
Cruise speed	121 kt	224 km/h
Max speed (at cruise)	173 kt	320 km/h

The aircraft ducted rotor is positioned aft of the cockpit and features an electrical RPM control with a fixed blade pitch angle. The forward tilt rotor pairs are counter-rotating and can be tilted forward and back. The aircraft is equipped with canards, and trailing-edge elevons on the main wing are provided. Moreover, the aircraft features rudders on the fin.

2.2. Aerodynamic Modelling

Figure 2 illustrates the modelling summary of the Volante Vision components.

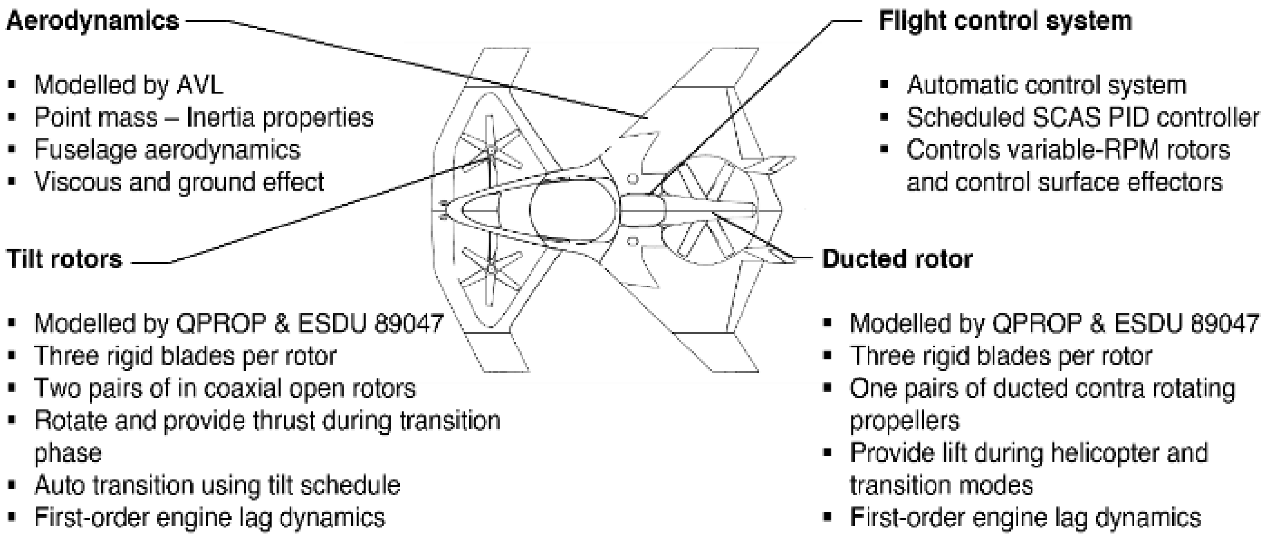

Figure 2 Schematic of the Volante Vision modelling components.

The Athena Vortex Lattice [19] method is used to analyse aerodynamic characteristics and derive the aerodynamic derivatives. The blade element momentum theory solver called QPROP [20] was used to predict the performance of the rotor thrust, along with semi-empirical corrections for coaxial rotors [21], neglecting viscous effects at high blade angle of attack. It is acknowledged that this ultimately degrades its fidelity when applied across the entire flight envelope. Moreover, considering that the predominant portion of downwash during the tilting phase occurs beneath the fuselage with minimal contact to the structure, the model disregards aerodynamic interference. The lift coefficient C_L, drag coefficient C_D, and pitching moment coefficient C_M are modelled in Equations from (1) to (3) based on the reference [22]. In these equations, C_{L_0} is the zero-lift coefficient, an C_{L_α} is the lift curve slope. C_{L_q} and C_{L_η} are lift coefficients due to pitch rate (q) and elevon deflection (η), respectively. C_{D_0} is the zero-lift drag coefficient, K is the lift-induced drag coefficient factor, C_{D_η} is the drag coefficient due to η, C_{M_0} is the zero-lift moment pitch coefficient, C_{M_α} is the pitching moment slope. C_{M_q} and C_{M_η} are pitch moment coefficients due to q and η, respectively. Together, these equations represent the aerodynamic coefficients as functions of the angle of attack α, pitch rate q, and elevon deflection η.

$$C_L = C_{L_0} + C_{L_\alpha}\alpha + C_{L_q}q + C_{L_\eta}\eta \tag{1}$$

$$C_D = C_{D_0} + KC_L^2 + C_{D_\eta}\eta \tag{2}$$

$$C_M = C_{M_0} + C_{M_\alpha}\alpha + C_{M_q}q + C_{M_\eta}\eta \tag{3}$$

2.3. Control Mechanism

Figure 3 shows longitudinal control effectors. In the low-speed hover configuration, both the ducted rotor and the tilt rotor pair collaborate to provide the necessary lift. Pitch and heave control is achieved through the differential and collective adjustment of the ducted and tilt rotor RPM speeds. Transitioning from the hover configuration to the fixed-wing aircraft configuration, and vice versa, is facilitated by varying the shaft tilt angle, i_T, thereby changing the direction of the fore rotor thrust vector. This strategy also contributes to surge control. In the fixed-wing aircraft configuration, the lifting surfaces generate sufficient aerodynamic lift to support the weight of the aircraft. Hence, the ducted rotor becomes redundant, and forward thrust is generated by the tilted fore rotors to move the aircraft. Moreover, in the fixed-wing operation condition, the main wing trailing-edge elevon is employed instead of the canard for pitch control in the fixed-wing aircraft configuration.

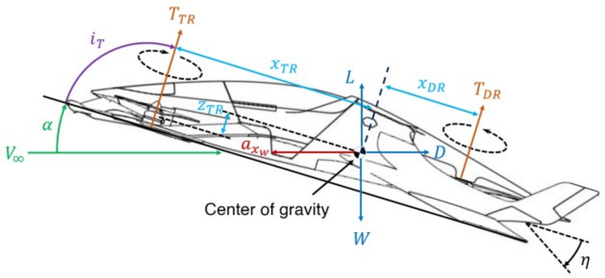

Figure 3 Longitudinal control effectors of the Volante Vision.

2.4. Actuator Dynamics

Incorporating the additional dynamics of components, such as motor lag and control surface actuator dynamics, is essential to model the stability and response characteristics of the aircraft augmented with FCS. Table 2 provides a detailed description of the model parameters for both actuator and motor dynamics.

Table 2 Actuator model parameters.

	Bandwidth (rad/sec)	Value limit	Rate limit (deg/sec)
Tilt motor	10	0 – 95 deg	9
Front motor	10	0 – 2500 rpm	
Rear motor	10	0 – 1800 rpm	
Elevon	30	±30 deg	90

The tilting actuator and motor lag dynamics are modelled as first-order systems with a bandwidth of 10 rad/sec, which is specifically selected to ensure that they are not intrusive in the overall system performance. The elevon control surface dynamics are represented as second-order systems, with a damping ratio of 0.75 and a bandwidth of 30 rad/sec. This bandwidth was derived from electro-mechanical actuator characteristics typically spanning from 3.5 to 8 Hz [23]. Typical rate limits for control surfaces reach the full actuator range per second [24]. However, to mitigate the risk of Category II Pilot-Induced Oscillations (PIO) due to rate or position limitations [25], a rate limit of 90 deg/sec was imposed in elevon actuator. A tilt rate limit of 6 deg/sec was implemented, reflecting HQ and minimum energy considerations, which are discussed in detail in the subsequent sections.

3. THEORITICAL BACKGROUND

3.1. Minimum Energy FCS Architecture

Figure 4 presents the overview of control response types and effector usage across the hover, transition, and cruise regimes of a tiltrotor eVTOL aircraft, distinguishing between longitudinal-axis control (LC) and heave-axis control (HC) channels. The architecture includes inner-loop stability and control augmentation to achieve Level 1 HQs. Detailed FCS design can be found in previous study [26].

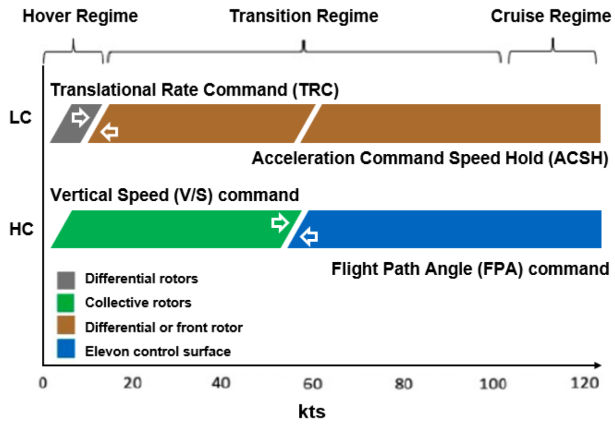

Figure 4 Overview of control response types and effector allocation.

3.2. Minimum Energy Command Profiles

Figure 5 presents the revised minimum-energy target command profiles for conversion and reconversion, updated based on the preferences and performance characteristics of flight-naïve pilots, in comparison to the baseline profiles in the previous study [9,26].

Both profiles incorporate a 0.2-second delay in the target command guidance indicator to compensate for pilot processing delay, as reported in previous studies [27]. Consequently, the actual target command is displayed with a 0.2-second lag relative to the current flight condition. In particular, the reconversion schedule has been modified to feature a more uniform deceleration segment, reflecting findings that constant acceleration profiles are associated with reduced subjective workload according to NASA TLX assessments [16]. The target command profiles for both conversion and reconversion were formulated to minimise pilot workload such that precise tracking of the guidance symbol inherently results in minimum-energy trajectories while simultaneously satisfying all desired performance criteria defined within the FTM evaluation metrics in Table C, which will be further discussed in the following section.

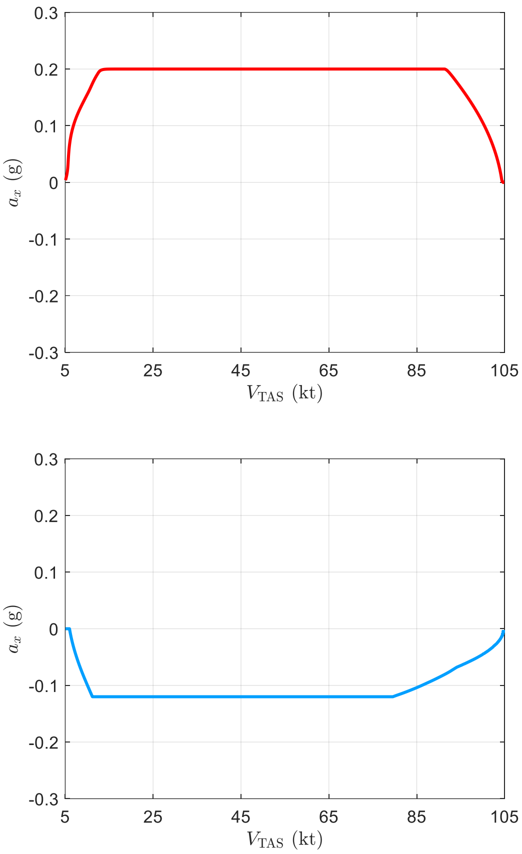

Figure 5 Minimum energy target command guidance profiles for conversion (top) and reconversion (bottom).

4. EXPERIMENTAL SETUP

4.1. Participants Background

Participants consisted of 12 individuals from three distinct background groups, classified based on their prior flight or simulation experience, as summarised in Table 3.

Table 3 Participant group classification by flight experience

Group	Experience Level	Participant Identifiers
A	No flight simulation experience	P1–P5
B	Prior flight simulation experience	P6–P10
C	Certified pilots	P11–P12

Group A included five participants with no flight simulation experience (P1 - P5), while Group B comprised five individuals with 2,770 prior average flight simulation experience hours (P6–P10). Group C consisted of two certified fixed-wing pilots (P11–P12) with 7,250 average flying hours.

4.2. Flight Simulation Facility

The Rolls-Royce Future Systems Simulator (FSS) at Cranfield University, shown in Figure 6, is a fixed-base research simulator offering medium- to high-fidelity capabilities, developed to support advanced studies in flight deck design, human factors, systems integration (mainly engine), and the experimental assessment of emerging aviation technologies within a controlled and repeatable test environment. Further technical details regarding the architecture, capabilities, and implementation of the FSS can be found in the reference [28].

The simulation inceptor hardware comprised a two-axis left-hand side-arm controller, thrust levers, and rudder pedals. As the study focuses on conversion and reconversion manoeuvres, lateral and directional control interfaces were not actively employed. Additionally, an autopilot function was engaged to maintain constant height throughout the manoeuvres, thereby isolating the test subject's task to longitudinal control. Participants were primarily required to use the left-hand inceptor, depicted in Figure 6, to track the minimum energy conversion and reconversion target command guidance. This inceptor configuration aligns with those adopted in previous eVTOL studies [29-31], including those conducted by NASA [11,32] and industrial developers such as Joby Aviation, Archer, etc. [33].

Figure 6 External and interior views of Rolls-Royce FSS.

4.3. Eye Tracking Device

The eye-tracking data in this study were collected using a lightweight, head-mounted device designed for high-precision binocular gaze tracking in both naturalistic and simulator-based environments, as illustrated in Figure 7 [34]. Specifically, the employed eye tracking device features a scene camera with a resolution of 1600 × 1200 pixels, a frame rate of 30 Hz, and a field of view of 103° × 77°. The system incorporates dual infrared eye cameras with a resolution of 192 × 192 pixels operating at a sampling rate of 200 Hz. It offers a spatial accuracy of 1.8° median angular error without user calibration, which can be improved to approximately 1.3° following a simple offset correction. The system also provides an intrinsic gaze stability noise of approximately 0.3° root mean square (RMS) during fixations. To evaluate pilot visual attention and cognitive workload during the conversion and reconversion manoeuvres, five specific eye-tracking parameters were selected: the number of blinks, and the proportion of fixation counts directed toward the target command guidance, pitch attitude and altitude indicators on the Primary Flight Display (PFD), and the external visual scene.

Figure 7 Eye tracking device used for fixation and blink analysis.

4.4. Development of Flight Test Manoeuvres

Table C outlines FTM in the study and associated performance criteria for evaluating conversion and reconversion phases during level flight. Evaluation metrics include minimum time constraints for completing conversion and reconversion, terminal airspeed accuracy, pitch attitude deviation, altitude deviation, etc. The criteria are categorised into desired and adequate standards, reflecting varying levels of pilot workload acceptability and control precision. The task is conducted across hover, conversion/reconversion, and aircraft modes, and is designed to assess HQs such as stability, agility, and comfort under minimum energy manoeuvring conditions. The objective of this FTM is to evaluate the aircraft ability to execute level flight accelerations and decelerations via automatic rotor tilting, while maintaining height and heading throughout the manoeuvre. The manoeuvre description specifies two distinct phases: conversion from hover to cruise, and reconversion from cruise to hover. During conversion, the aircraft initiates a longitudinal acceleration to reach 105 knots while holding altitude with a constant pitch attitude; reconversion follows the inverse sequence, decelerating from cruise to a stabilised hover.

4.5. Target Command Guidance System

For the assessment of manually flown minimum-energy trajectories, test subjects were provided with a PFD incorporating a target command guidance indicator. Figure 8 illustrates the PFD interface used during the conversion and reconversion FTMs. The minimum-energy guidance cues were integrated into the head-down display to simulate Instrument Meteorological Conditions (IMC). In good visual environments (GVE), the same guidance would ideally be presented on a head-up display (HUD) to support more effective pilot workload allocation.

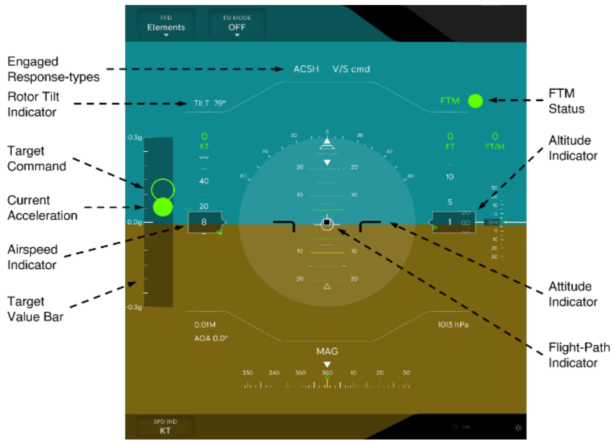

Figure 8 Head-down display used for conversion/reconversion FTMs.

4.6. Procedure

Table 4 summarises the experimental procedure and task timeline for the piloted simulation study. The protocol was structured into five sequential stages: Introduction, Brief, Familiarisation, Flight Simulation, and Debrief, with an overall session duration of approximately 110 minutes. During the Introduction phase (5 minutes), participants were asked to sign a consent form and complete a demographic survey. This was followed by a Briefing session (15 minutes), where participants reviewed the eVTOL model, flight control mechanisms, the PFD, and FTM involving conversion and reconversion. The Familiarisation phase (30 minutes) allowed participants to conduct a practice simulation flight to become accustomed to the scenario and controls. The main Flight Simulation task (30 minutes) required participants to perform the conversion/reconversion FTM under experimental conditions. Each participant completed three consecutive attempts, either with or without the target command guidance system at each, depending on the assigned test condition. In the absence of guidance, participants were briefed on the energy optimal profiles and the derivation of Figure 5, enabling them to regulate the current acceleration in an attempt to infer and follow the minimum energy trajectory based on their understanding of the dynamics. This was conducted under the supervision of both a flight instructor and an eye-tracking operator. Objective performance measures, such as task time and simulator-logged flight parameters, were recorded. In setups referencing prior research protocols, additional data such as eye-scan patterns, video recordings, and verbal protocol data were also collected. In the final Debrief stage (30 minutes), participants completed the NASA-TLX to assess perceived workload and a comfort rating survey, shown in Appendices A and B, along with qualitative feedback on their flight experience.

Table 4 Experimental procedure and task timeline for piloted simulation study.

Task	Description	Duration
Introduction	Participants are asked to sign a consent form and complete a demographic survey.	5 min
Brief	Participants review the eVTOL model, flight control mechanism, PFD, and conversion/re-conversion FTM.	15 min
Familiarisation	Participants practice flight simulations for task familiarisation.	30 min
Flight simulation	Participants perform conversion/re-conversion FTM trials with or without target command guidance system.	30 min
Debrief	Participants complete NASA-TLX and comfort rating survey and provide feedback on their flight simulation experience.	30 min

5. SIMULATION RESULTS

The primary objective of this study was to demonstrate a conversion and reconversion flight profile that is both easy to perform and comfortable for the pilot, while also achieving minimum energy consumption as outlined in the preceding section. The results indicated that all participant groups were able to successfully complete the conversion and reconversion manoeuvres under the defined experimental conditions. This conclusion is substantiated by objective metrics, including the deviation from energy-optimal trajectories and cognitive workload indicators derived from fixation and blink parameters, as well as by subjective measures such as NASA TLX workload assessments and participant comfort ratings. The following section presents a detailed analysis of the results, accompanied by discussions of key performance trends, workload implications, and the influence of guidance augmentation.

5.1. Comparison of Objective Ratings

a. Conversion FTM Evaluation

Figure 9 to Figure 16 present the piloted simulation results for the conversion manoeuvre conducted with/without the target command guidance system. The conversion profile is segmented into three characteristic phases, denoted as P_1, P_2, and P_3. Phase P_1 begins immediately after the automatic control system transitions into ACSH mode, aligning all participant results from a consistent initial condition. This phase corresponds to the initial acceleration segment, where the longitudinal acceleration increases up to approximately 0.2 g within the first 5 seconds. Phase P_2 represents the intermediate segment of the manoeuvre, during which a nearly constant acceleration is maintained to reach a cruise speed of approximately 105 kt. Phase P_3 denotes the final segment, in which the pilot decelerates the aircraft to complete the conversion manoeuvre at the desired terminal airspeed range according to FTM.

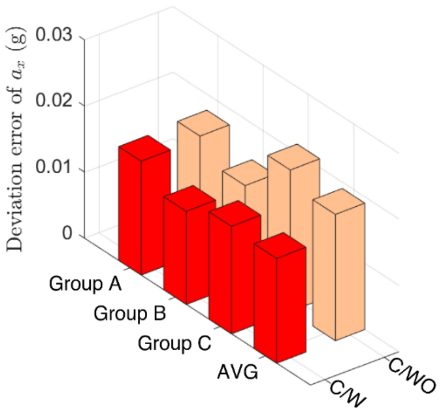

Figure 9 Deviation error against minimum energy trajectory during conversion (C) FTMs with (W) and without (WO) target command guidance.

As shown in Figure 9, the acceleration deviations from the desired command reference profile depicted in Figure 5 were small enough for the majority of test subjects to meet the desired criteria of conversion FTMs. Specifically, minimum energy conversion trajectories flown with the target command guidance system demonstrated superior performance compared to those flown without guidance. This was evidenced by reduced deviations from the desired minimum-energy acceleration profiles and a higher level of compliance with the defined performance criteria outlined in the FTM specification.

Figure 10 illustrates the mean longitudinal inceptor inputs applied by the three participant groups throughout the conversion manoeuvre.

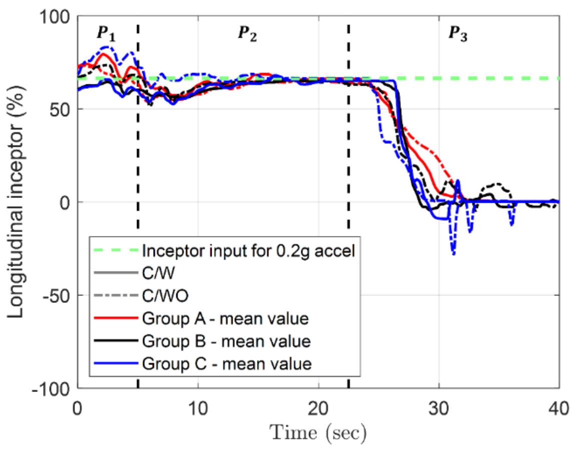

Figure 10 Longitudinal inceptor inputs during conversion introduced by 12 test subjects.

During Phase P_1, the majority of participants increased their inceptor input to approximately 66%, which aligns with the inceptor input required to generate the target acceleration of 0.2 g, as shown in Figure 5. This anticipatory behaviour reflects participants' understanding that the control interface dynamics include a rate limiter of 0.05 g/sec, and that prompt acceleration build-up is essential to align with the minimum-energy trajectory.

It was Phase P_2 where most of the deviation in Figure 9 occurred, as shown in Figure 11. As Phase P_2 begins, any inceptor input resulting in acceleration above 0.2 g intensifies control sensitivity due to the steep segment of the conversion tilt schedule. Specifically, beyond a rotor shaft angle of 55 deg, the schedule is configured to produce a tilt rate of 6 deg/s only when acceleration remains at 0.2 g. If higher acceleration is applied while the tilt schedule remains locked to airspeed, the resulting tilt rate exceeds the intended 6 deg/sec and reaches up to 8.5 deg/sec, as shown in Figure 12. This elevated tilt rate increases control sensitivity, making the aircraft more responsive to small inceptor inputs. This effect is visible in Figure 13, where some participants exhibited acceleration levels reaching up to 0.3 g during early Phase P_2. This led to notable deviations from the desired FTM criteria in the unguided condition, as evidenced by the pitch attitude variations in Figure 14 and the acceleration discrepancies in Figure 11. The target command guidance system was shown to mitigate this effect by enabling participants to better regulate inceptor inputs and maintain acceleration closer to the 0.2 g target.

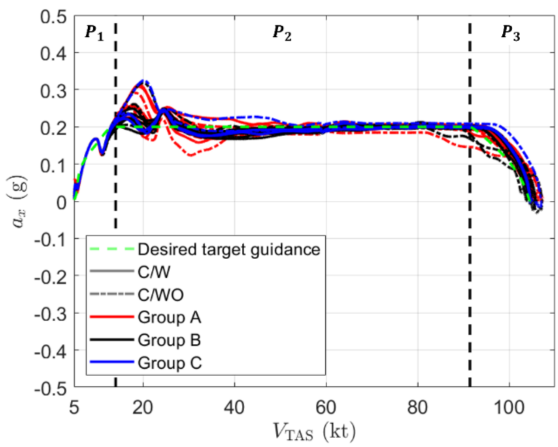

Figure 11 Conversion profile comparison between the desired target command and piloted simulation results.

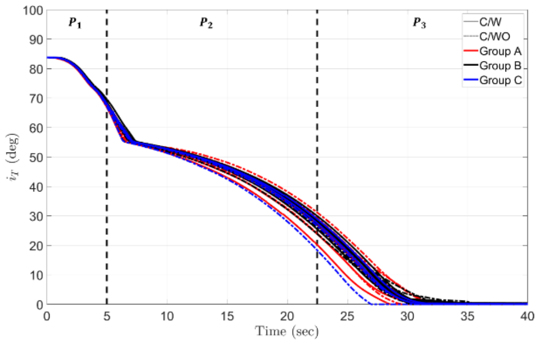

Figure 12 Rotor shaft angle response during conversion FTM across experimental groups with/without guidance.

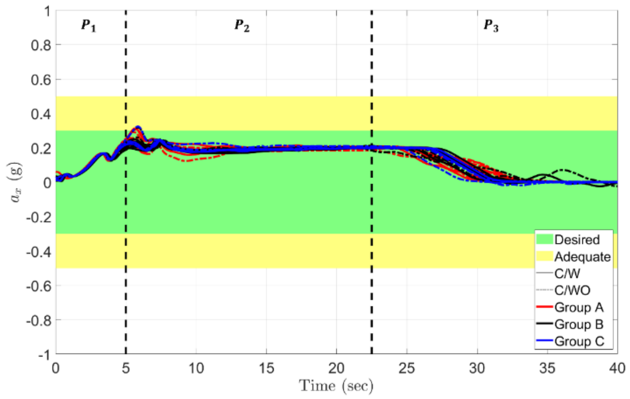

Figure 13 Acceleration response during conversion FTM across experimental groups with/without guidance.

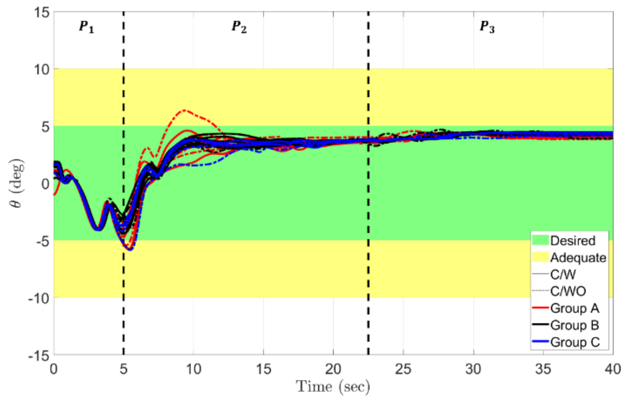

Figure 14 Pitch attitude response during conversion FTM across experimental groups with/without guidance.

Moreover, the opposite issue becomes more pronounced when modulating the inceptor input to reduce acceleration. This asymmetry arises because pushing the inceptor forward continuously lowers the rotor shaft angle, which contributes to increased acceleration. Consequently, pulling the inceptor back to achieve decreasing acceleration becomes less effective due to the altered control sensitivity induced by the changing tilt dynamics. This disparity in control sensitivity is reflected in Figure 11, where acceleration deviations above the target were larger than those below. Such non-uniform sensitivity aligns with feedback, particularly from Group C, which noted that "current acceleration does not move linearly." Once the shaft angle drops below 55 degrees in Phase P_2, the tilt schedule transitions to a more gradual slope, thereby alleviating the control sensitivity issues observed earlier in the manoeuvre. The observed improvement in control sensitivity and HQ associated with a lower tilt rate is consistent with the findings reported in the reference [24].

In Phase P_3, deceleration is applied to bring the airspeed down to the FTM-specified terminal speed of 105 kt (±2 kt). The steep slope of the tilt schedule does not exacerbate control sensitivity in this phase, because the declining acceleration inherently results in a reduced tilt rate. As shown in Figure 15, most participants, except for a few, especially in unguided trials, successfully met terminal airspeed targets. Throughout all phases, altitude remained within desired limits due to autopilot height-hold engagement, referring to Figure 16.

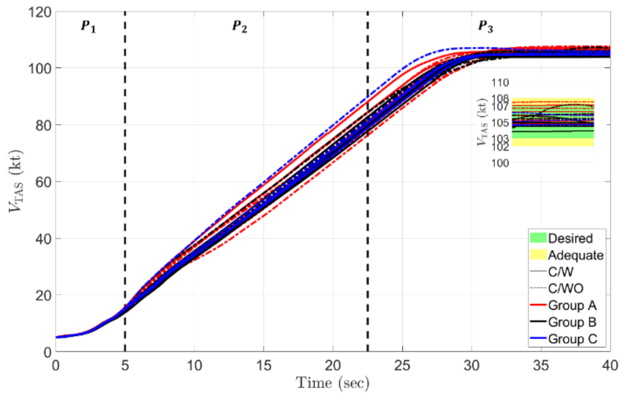

Figure 15 True airspeed response during conversion FTM across experimental groups with/without guidance.

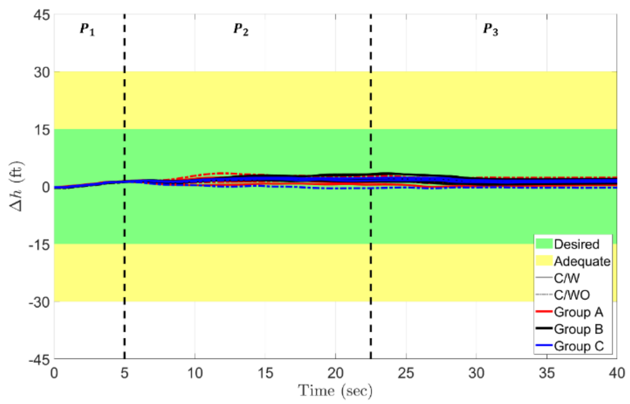

Figure 16 Height response during conversion FTM across experimental groups with/without guidance.

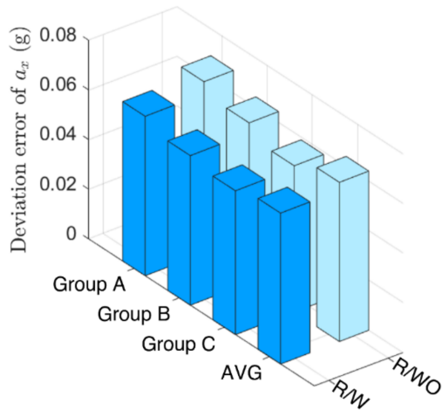

Figure 17 Deviation error against minimum energy trajectory during Reconversion (R) FTMs with/without target command guidance.

b. Reconversion FTM Evaluation

Figure 17 to Figure 24 present the simulation results for reconversion FTMs, conducted with/without the aid of target command guidance systems. Each phase of the reconversion trajectory is segmented into three characteristic regions, labelled P_1 to P_3. The first region, P_1, corresponds to the initial deceleration build-up, reaching approximately −0.12 g over a duration of 20 sec. This is followed by P_2, representing the phase of sustained constant deceleration before the aircraft approaches near-hover speeds of 5 kt. The final segment, P_3, captures the termination phase of the reconversion manoeuvre, in which deceleration is further modulated to settle the airspeed at the designated terminal value. Overall, as shown in Figure 17, the deceleration deviations from the desired command reference profile depicted in Figure 5 were low enough for test subjects to achieve the most desired criteria of reconversion FTMs. In particular, minimum-energy reconversion trajectories flown with the target command guidance system demonstrated superior performance compared to those flown without the guidance symbol. This was evidenced by reduced deviations from the desired minimum energy deceleration profiles and a higher level of compliance with the performance criteria defined in the FTM specification.

Figure 18 illustrates the mean longitudinal inceptor inputs applied by the three participant groups throughout the reconversion manoeuvre. During Phase P_1, continuously pulled back the inceptor for approximately 20 seconds, reaching around -40%. This target deceleration value corresponds to the inceptor input required to achieve the target deceleration of -0.12 g, as defined in the minimum-energy trajectory shown in Figure 5.

Most of the deviation observed in Figure 17 is primarily attributed to Phase P_1, as corroborated by the trend illustrated in Figure 19. This is further supported by the wide variation in rotor shaft angle prior to reaching 95 degrees, as illustrated in Figure 20, which reflects the differing deceleration command trends depicted in Figure 21. These variations ultimately result in the pitch attitude deviations shown in Figure 22, particularly under unguided conditions. This was not only due to the piloting challenge associated with tracking a continuously changing deceleration target during reconversion, but also due to the adverse impact on FCS performance when participants failed to precisely track the target command guidance. Specifically, imprecise tracking leads to flying outside the conditions for which neutral control input mapping, illustrated in previous study [26], was designed, thereby degrading FCS performance.

The resulting mismatch is most clearly reflected in the two major deceleration deviation peaks seen in Figure 19. The first peak corresponds to the point at which the system transitions to RPM-based control, where neutral mapping of the elevon becomes active. The second peak is associated with the cessation of tilt rate changes, which had previously acted as a dynamic disturbance, coupled with the accumulated deviation from the intended flight condition for which the neutral control input mapping was designed.

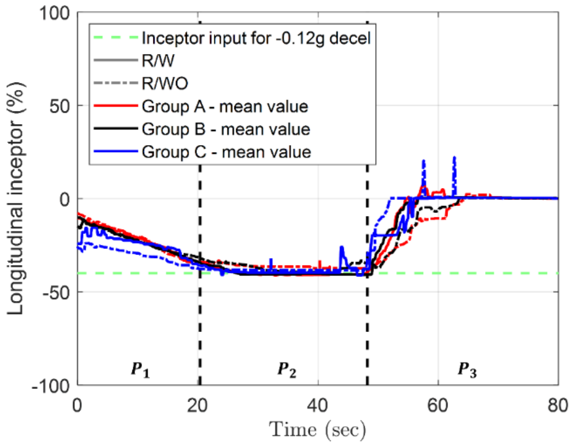

Figure 18 Longitudinal inceptor inputs during reconversion applied by 12 test subjects.

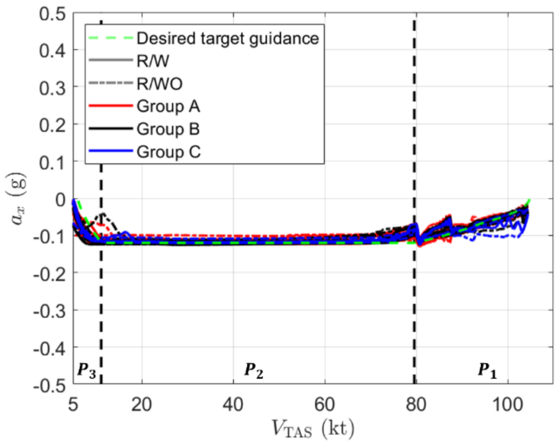

Figure 19 Reconversion profile comparison between the desired target command and piloted simulation results.

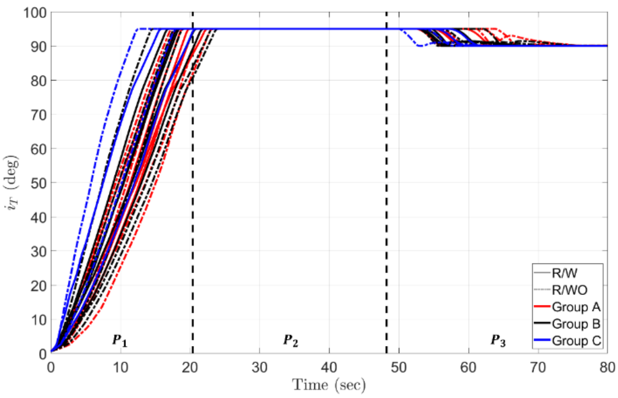

Figure 20 Rotor shaft angle response during reconversion FTM across experimental groups with/without guidance.

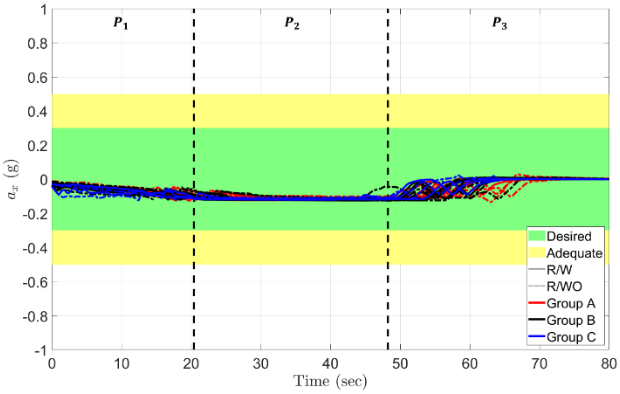

Figure 21 Acceleration response during reconversion FTM across experimental groups with/without guidance.

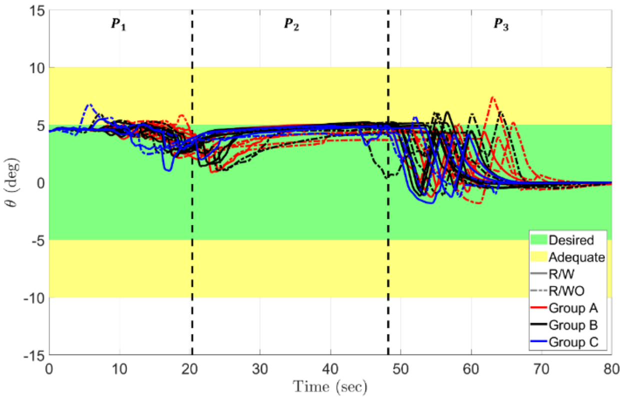

Figure 22 Pitch attitude response during reconversion FTM across experimental groups with/without guidance.

In contrast, this control coupling issue related to neutral input mapping was negligible during the conversion manoeuvre. At lower speeds, particularly far below stall conditions, conversion flight relies more heavily on powered thrust, limiting the range of operational flight conditions and thus minimising deviation from those designed for neutral control mapping. Conversely, during reconversion, a broader spectrum of flight conditions remains viable, even at constant deceleration, due to the combined use of powered and aerodynamic control. As a result, the FCS during reconversion is more susceptible to performance degradation when deviating from the prescribed flight regime. This disparity accounts for the substantially higher mean deviation error observed in reconversion (Figure 17) compared to conversion (Figure 9).

However, the control sensitivity issue attributed to the tilt schedule, which was evident during conversion, did not manifest in the reconversion manoeuvre, despite both phases employing the same designed maximum tilt rate of 6 deg/sec. This discrepancy can be explained by fundamental differences between the aerodynamic and propulsion requirements in conversion and reconversion. During conversion, tilting beyond 55 degrees occurs below around $0.25V_S$, necessitating a high proportion of powered lift rather than aerodynamic lift. Additionally, as conversion flight involves positive acceleration, further thrust must be generated and redirected via rotor tilting. This coupling between large thrust magnitudes and tilt rate variations amplifies the control sensitivity. In contrast, reconversion occurs at relatively lower thrust demands. For instance, at a rotor shaft angle of 60 degrees, the total required thrust during reconversion is approximately 27% of that required during conversion. This difference in thrust magnitude means that even with the same nominal tilt rate, the dynamic coupling between the tilt mechanism and the aircraft response is further alleviated in reconversion with no observable control sensitivity issue.

In Phase P_2 of the reconversion manoeuvre, a constant maximum deceleration is commanded by leveraging the horizontal force component of the powered thrust, while maintaining the rotor shaft angle at approximately 95 deg. This segment is designed to reduce airspeed efficiently before transitioning to the final phase. During P_3, participants are tasked with terminating the reconversion precisely at 0 kt, within the terminal airspeed boundary of ±2 kt as defined in the FTM. As the airspeed drops below 5 kt, a discrete 5 deg step reduction in rotor shaft angle is commanded, shifting it from 95 degrees back to 90 degrees. To avoid a sudden pitch-up motion resulting from this change due to the FCS compensation, a steady rotor shaft angle reduction strategy was applied to mitigate abrupt attitude disturbances. This control approach is reflected in the observed increases in deceleration and pitch attitude in Figure 21 and Figure 22, respectively.

However, in unguided trials, some participants continued to pull back on the inceptor during the automatic transition from ACSH to Translational Rate Control (TRC), unintentionally commanding negative airspeed, while appropriate for deceleration in ACSH. When this input was combined with the maximum deceleration rate of −0.12 g and the step input rotor shaft angle control strategy, it often led to overshooting or delayed convergence to the desired terminal speed, particularly in the absence of target command guidance, as illustrated in Figure 23 and Figure 20.

Despite these challenges, altitude control was consistently maintained within desired boundaries throughout all reconversion phases due to the active engagement of the autopilot height-hold function, as shown in Figure 24.

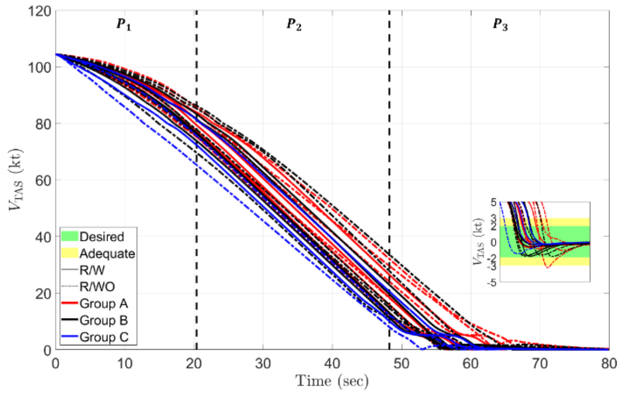

Figure 23 True airspeed response during reconversion FTM across experimental groups with/without guidance.

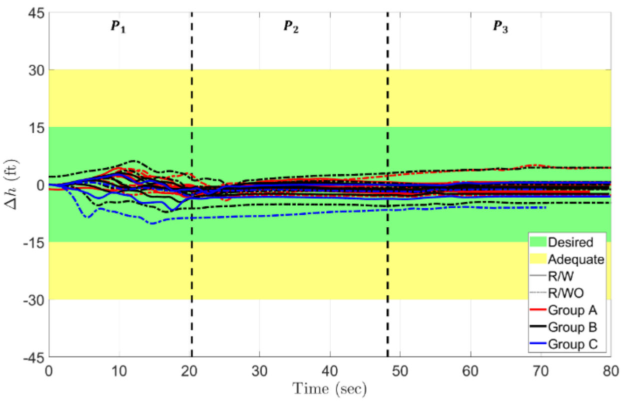

Figure 24 Height response during reconversion FTM across experimental groups with/without guidance.

5.2. Comparison of Subjective Ratings

Figure 25 and Figure 26 present the average normalised NASA TLX workload and comfort ratings reported by all test participants across three groups (A, B, C). The "AVG" column indicates the average rating across the three groups for each condition. Overall, all average NASA TLX workload ratings remained as a low workload below 50%. Particularly, conversion and reconversion scenarios involving the target command guidance system consistently yielded the lowest workload ratings. In addition to TLX ratings, all comfort ratings were recorded high at around 80% across all the groups.

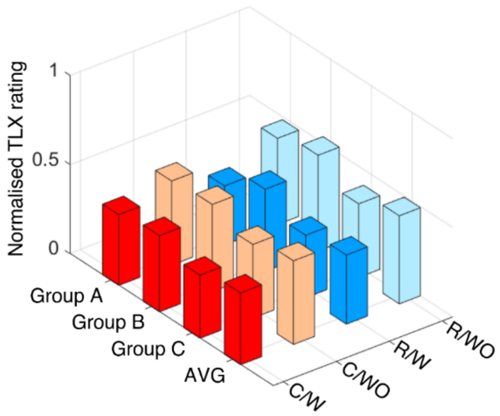

Figure 25 Normalised NASA TLX ratings across participant groups and experimental conditions.

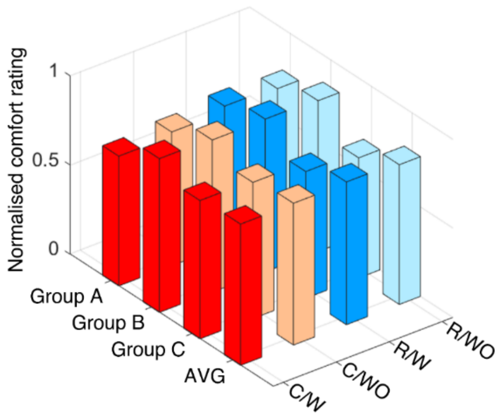

Figure 26 Normalised comfort ratings across participant groups and experimental conditions.

5.3. Comparison of Cognitive Workload

a. Fixation Evaluation

A fixation, in the context of cognitive psychology, refers to the brief interval during which the eyes remain relatively stationary, focusing on a specific visual element. Fixations are key indicators of where and how visual attention is allocated during a task. Fixation count (the number of discrete fixations) and fixation duration (the average time spent per fixation) are two fundamental metrics commonly employed to infer cognitive workload, visual scanning behaviour, and task engagement.

Figure 27 provides a representative example of fixation behaviour recorded by the eye-tracking system during the conversion and reconversion manoeuvres. Fixation data were categorised across predefined Areas of Interest (AOIs), specifically the external view (AOI-1), target command guidance indicator (AOI-2), attitude display area (AOI-3), and altitude indicator (AOI-4). Each fixation event is depicted as a circle, with its radius corresponding to the fixation duration, while the associated fixation count is displayed adjacent to the gaze point. In this particular instance, the participant briefly fixated on the external scene in AOI-1 before directing visual attention from the rotor shaft angle region in AOI-3 to the target command guidance symbol in AOI-2.

Figure 28 and Figure 29 reveal how fixation metrics—average fixation duration and number of fixations—varied across different visual interface areas during conversion and reconversion FTMs for three groups. Overall, the Target Command Guidance area consistently elicited the highest fixation durations and fixation counts across all AOIs and manoeuvres. This suggests that participants placed substantial trust in the acceleration indicator as a reliable reference for achieving minimum-energy trajectories and satisfying the desired FTM performance criteria. Notably, conditions involving guidance (C/W and R/W) induced higher cognitive workload—manifested as longer fixation times during conversion and higher fixation counts during reconversion—compared to unguided conditions. This elevated visual and cognitive engagement aligns with reduced deviation from the ideal minimum-energy trajectory observed in Figure 5, reflecting a performance-effort trade-off.

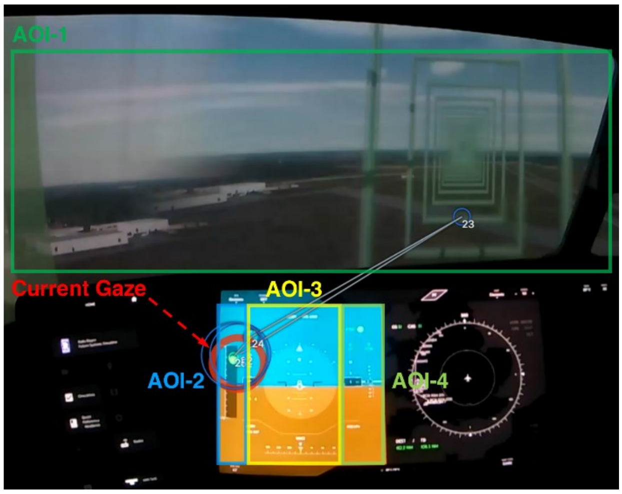

Figure 27 Sample fixation mapping output from the eye tracking device.

More specifically, the increased cognitive workload observed during Phase P_2 of the conversion manoeuvre appears to be a significant contributor to prolonged fixation durations. During this phase, the control sensitivity intensifies due to the steep segment of the conversion tilt schedule. The tilt rate of 6 deg/s is only guaranteed if the commanded acceleration is precisely 0.2 g before the rotor shaft angle reaches approximately 55 deg, as shown in Figure 12. Even minor positive deviations in inceptor input relative to the optimal acceleration result in tilt rates exceeding 6 deg/sec, producing higher-than-expected acceleration. Furthermore, the non-differentiable slope of the tilt schedule near the 55 deg transition point results in an abrupt change in control sensitivity. Following this point, the tilt rate drops, leading to a smoother conversion phase. These transitions in the tilt schedule require test subjects to actively monitor and continuously compensate for their control inputs, thereby imposing a higher cognitive workload, particularly during the early portion of Phase P_2. This is supported by eye-tracking metrics showing elevated fixation activity in this interval.

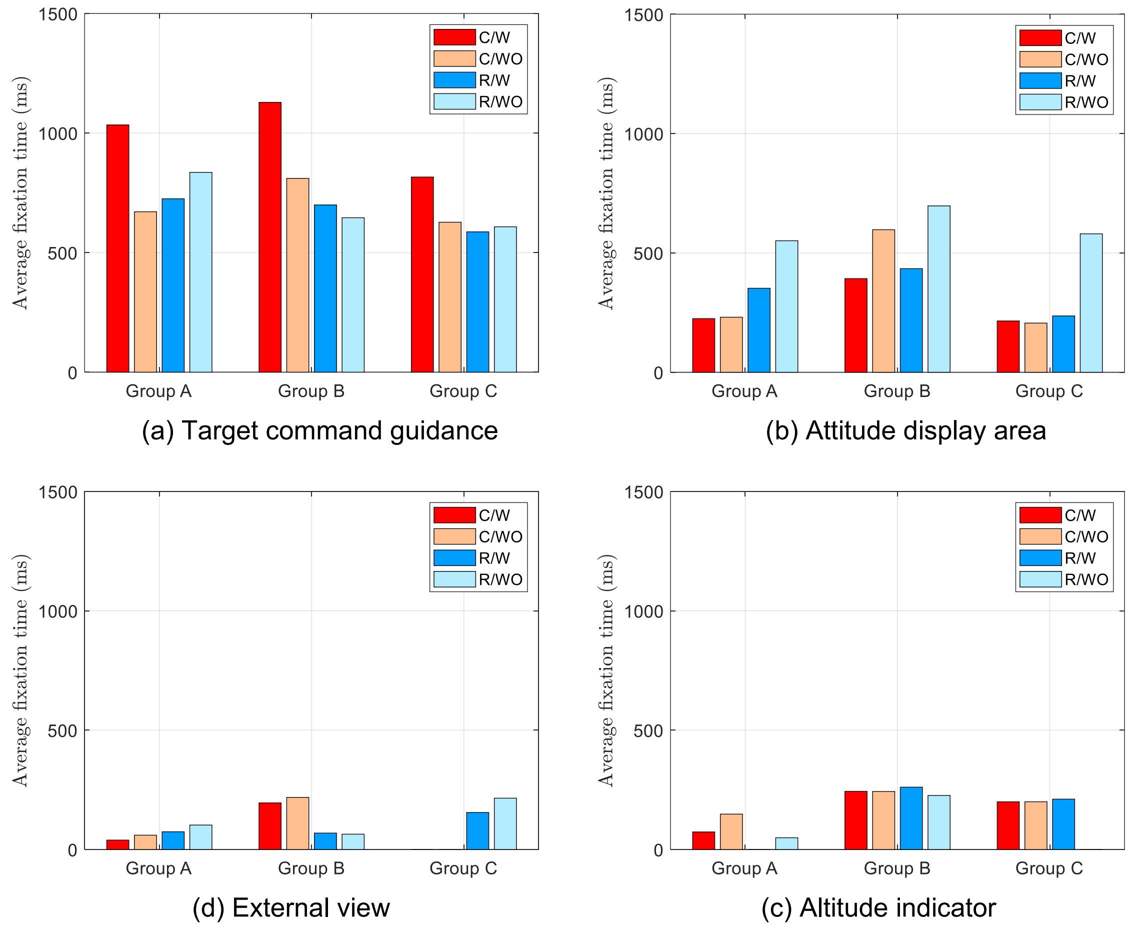

Figure 28 Average fixation time across visual interface during conversion and reconversion FTMs.

When it comes to reconversion, it was Phase P_1 that accounted for the majority of the observed fixation counts. This segment involved a continuously increasing target deceleration command over a prolonged duration of approximately 20 seconds, aiming to reach −0.12 g prior to attaining a rotor shaft angle of 95 deg. The need for sustained visual monitoring and precise input adjustments during this phase imposed a cognitive demand on the participants, resulting in the highest fixation activity among the three reconversion phases (P_1 to P_3). This was consistent with test subject comments indicating that they were aware the maximum applicable deceleration was tightly constrained to remain within a reasonable pitch attitude range for passenger comfort, particularly before reaching a rotor shaft angle of 95 deg.

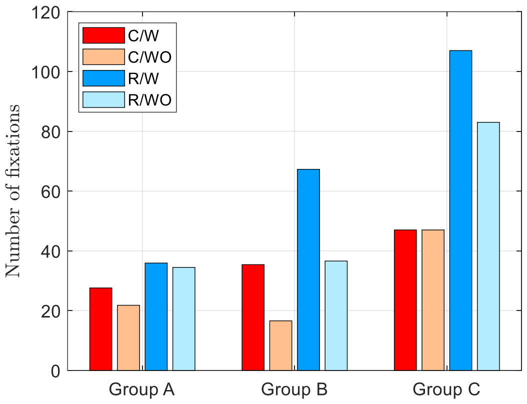

(a) Target command guidance

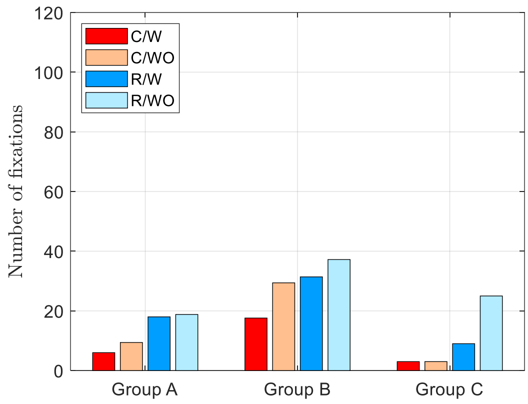

(b) Attitude display area

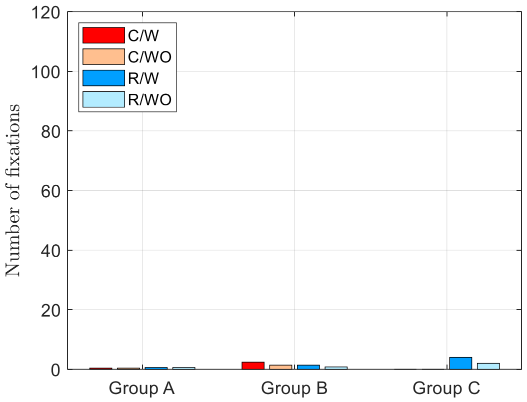

(c) Altitude indicator

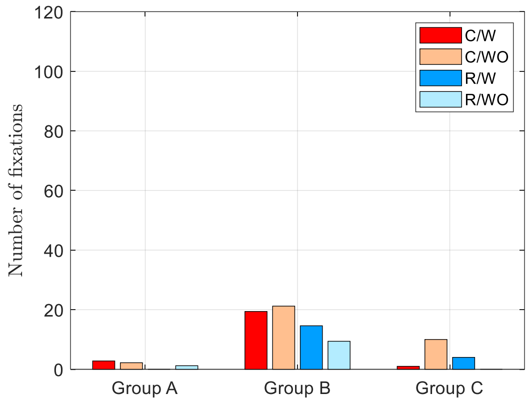

(d) External view

Figure 29 Number of fixations across visual interface during conversion and reconversion FTMs.

b. Blinks Evaluation

Figure 30 and Figure 31 present comparative results of blink-related metrics during conversion and reconversion, namely, the total number of blinks and average blink duration, across three participant groups under two experimental conditions: with/wtihout target command guidance. These blink metrics provide valuable insight into the pilot's attentional state and cognitive workload level during flight manoeuvres. Blink duration reflects the level of visual focus and alertness during task execution, with shorter durations typically indicating higher visual attention or engagement. In contrast, the number of blinks serves as an indicator of cognitive workload and stress. A higher frequency of blinks is generally associated with increased mental effort, fatigue, or stress, as the cognitive system attempts to regulate and cope with task demands.

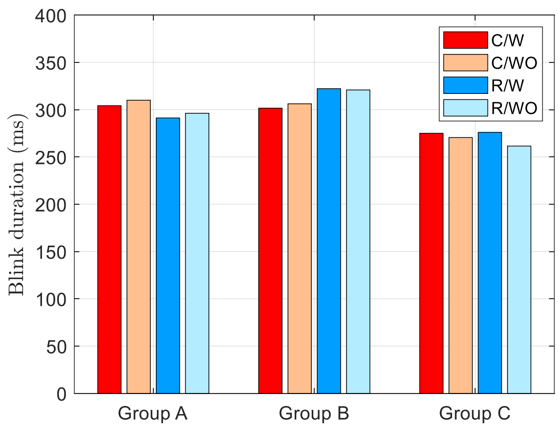

Figure 30 Average blink duration across experimental groups during conversion and reconversion FTMs.

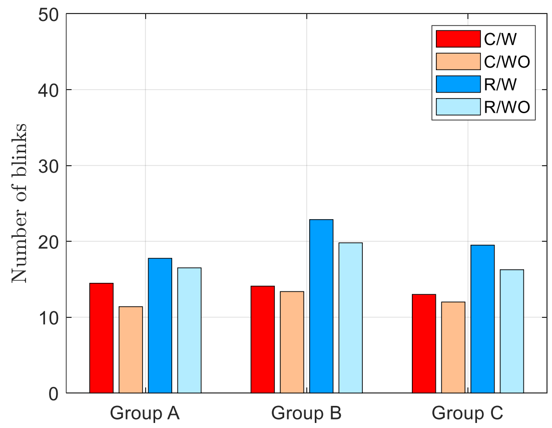

Figure 31 Number of blinks across experimental groups during conversion and reconversion FTMs.

Overall, the average blink duration remained consistent across all participant groups, not exceeding the average healthy benchmark of 334 ms [35]. This suggests that, from a visual engagement perspective, the task did not impose excessive strain, which aligns with the comfort rating outcomes presented in Figure 26. However, despite the similarity in blink duration, a noticeable increase in blink frequency was observed in both conversion and reconversion manoeuvres when the target command guidance system was employed. This elevated blink rate suggests that participants experienced greater cognitive workload and stress in the guided conditions compared to trials without the guidance symbol. The observed increase is attributable to the additional cognitive demand associated with managing nonlinear control sensitivity during the conversion phase and tracking the prolonged, gradually changing target command during the reconversion phase. These interpretations are supported by the fixation durations and counts presented in Figure 28 and Figure 29.

5.4. Discussion

The central objective of this research was to evaluate whether minimum-energy trajectories are both comfortable and manageable for flight-naïve pilots. This question was addressed through a comprehensive analysis of objective performance metrics and subjective workload and comfort ratings. The results demonstrate that deviations from the target command profiles were generally low enough across all groups and trials to meet the majority of the FTM desired criteria. These findings are corroborated by low average scores on the NASA TLX workload assessments and consistently high comfort ratings.

Performance outcomes, however, exhibited a dependence on the availability of target command guidance. Participants assisted by the guidance system achieved higher compliance rates with FTM desired criteria, 92% for both C/W and R/W, compared to 66% for C/WO and only 42% for R/WO. These results underscore the importance of target command guidance augmentation in facilitating successful adherence to minimum-energy trajectories and meeting desired criteria defined in the FTM, particularly in reconversion scenarios. The R/WO condition yielded the lowest success rate, primarily due to pitch attitude deviations exceeding the 5 deg limit, which was triggered by the automatic transition from ACSH to TRC. Participant feedback highlighted the need for consistent response characteristics during reconversion. This suggests that providing pilots with the manual engagement or disengagement of ACSH and TRC modes near hover speed may mitigate confusion and improve HQ. With the aid of the target command guidance system, 92% of participants from all groups, irrespective of prior background, successfully tracked minimum-energy transition strategies and met the desired criteria defined in the FTM. This directly addresses the research objective and affirms the suitability of the proposed approach. Nonetheless, aspects of the control design and trajectory formulation may require further refinement to reduce cognitive workload.

From the transition trajectory design perspective, minimum-energy transition strategies in conversion require a prompt reduction of the rotor shaft angle, and the associated tilt schedule induces varying control sensitivity that prevents pilots from forming reliable expectations about control input-response characteristics. These issues suggest that the tilt schedule should be constructed to ensure differentiability at least with respect to airspeed and shaft angle, and incorporate more gradual slopes to mitigate abrupt sensitivity changes. While such modifications would help mitigate abrupt sensitivity changes, they would inherently compromise the minimum-energy mechanism, particularly in the conversion phase. For reconversion, the gradual increase of target command guidance during Phase P_1 was perceived as demanding, especially compared to the constant deceleration phase that followed. This challenge stems from the requirement to track an incrementally increasing deceleration profile over approximately 20 seconds prior to reaching a shaft angle of 95 deg, under the constraint of maintaining pitch attitudes below 5 deg for passenger comfort. Test subject feedback, particularly from Group C, indicated that a gradual increase in target command over such an extended duration is impractical in operational flight scenarios, where pilots must also manage concurrent tasks. This further supports the recommendation to implement an acceleration-hold function, even for constant acceleration/deceleration profiles. This observation suggests that, given aerodynamic drag dominates more deceleration before 95 deg, initiating reconversion at a higher airspeed, where the −0.12 g target is immediately attainable, could enable the use of a constant deceleration profile from the outset. It is proposed that reconversion commence with pitch attitudes below the maximum 5 deg limit, in contrast to the current scheme where attitude remains saturated throughout the manoeuvre. However, initiating reconversion at higher speeds as a means of enabling immediate application of a constant deceleration profile entails operating under high advance ratio conditions. Such conditions may adversely impact propulsion system efficiency due to increased rotor aerodynamic losses and potential degradation in power effectiveness. Therefore, while this approach may enhance HQ and reduce pilot workload, it introduces an additional trade-off that compromises the energy-optimality of the reconversion strategy.

From a human factors standpoint, a large volume of fixations were made on the target command guidance across all three groups during the four scenarios, compared to the fixations made on the remaining three AOI's. The results indicate that, while participants achieved a higher compliance rate with the target guidance system activated, the expenditure of attention to the expense of other AOI's indicates a potential loss of situational awareness in operators while managing the conversion/reconversion manually. In periods of high cognitive workload, the lack of fixations detected in the study for all flight parameters revealed a potential design flaw, which would draw too much attention from participants during the proposed conditions. While the scanning behaviour can be attributed to the experience and exposure of participants to the eVTOL, the distribution of fixations indicates a bottleneck in cognition which could prevent sufficient scanning of the flight environment and terrain clearance during low-level flight. This could be resolved by utilising an audio chime when pilots are receiving the allotted flight profile for either conversion or reconversion flight, which can divert some visual attention to flight altitude and conflict detection monitoring. Additionally, heads-up display can be further incorporated with the target command guidance to promote a better heads-up philosophy for eVTOL operators, especially in GVE, as well as providing intuitive information presentation to pilots operating in this scenario.

6. CONCLUSIONS

This study has evaluated the feasibility of minimum-energy transition trajectories for vectored-thrust eVTOL aircraft in piloted operation by flight-naïve users. The results indicate that, under experimental conditions, both conversion and reconversion manoeuvres were successfully performed by participants with varying levels of flight experience, particularly when aided by a target command guidance system. Objective tracking errors remained within thresholds defined by the FTM desired criteria along with eye-tracking indicators, and subjective measures, such as workload ratings and, comfort assessments, affirmed the usability of the proposed control and guidance architecture. From the results obtained in this study, the following conclusions have been established:

- The guidance system significantly improved pilot task performance, increasing FTM compliance from 66% and 42% in unguided conversion and reconversion to 92% in both guided cases.
- Subjective assessments using the NASA TLX and comfort ratings revealed overall low workload below 50% and high comfort above 80% for minimum energy transitions phases.
- During conversion, rapid rotor shaft angle changes inherent to the minimum-energy tilt schedule resulted in variable control sensitivity, which challenged pilot expectations and response predictability.
- Differentiable tilt profiles with smoother gradients can further improve minimum energy conversion, even if such modifications compromise absolute energy-optimality.
- In reconversion, the gradual increase in deceleration command prior to tilt saturation imposed sustained cognitive effort over approximately 20 seconds, which was reported as demanding by pilot participants.
- Reconversion profiles can be further enhanced by beginning at higher airspeeds where constant deceleration targets are immediately achievable,

while such modifications may incur aerodynamic and power efficiency penalties.

- Supplementary auditory cues and heads-up display HUD integration are recommended to offload visual demand and promote better scan behaviour.

Namuk Kang Namuk.Kang@cranfield.ac.uk

Linghai Lu L.Lu@cranfield.ac.uk

James Whidborne j.f.whidborne@cranfield.ac.uk

Declan Saunders Declan.Saunders.173@cranfield.ac.uk

Wen-Chin Li wenchin.li@cranfield.ac.uk

REFERENCES

1. Doo, J. T., Pavel, M. D., Didey, A., Hange, C., Diller, N. P., Tsairides, M. A., Smith, M., Bennet, E., Bromfield, M., and Mooberry, J., "NASA Electric Vertical Takeoff and Landing Aircraft Technology for Public Services–A White Paper," NASA, 2021.
2. Rajendran, S., and Srinivas, S., "Air Taxi Service for Urban Mobility: A Critical Review of Recent Developments, Future Challenges, and Opportunities," Transportation Research Part E: Logistics and Transportation Review, Vol. 143, No. C, 2020, p. 102090. https://doi.org/10.1016/j.tre.2020.102090
3. Yang, X.G., Liu, T., Ge, S., Rountree, E., and Wang, C.Y., "Challenges and Key Requirements of Batteries for Electric Vertical Take-off and Landing Aircraft," Joule, Vol. 5, No. 7, 2021, pp. 1644–1659. https://doi.org/10.1016/j.joule.2021.05.001
4. Berger, T., Bridges, D., Hagwood, G., Miller, D., and Horn, J., "Piloted Simulation Evaluation of Damage Tolerant Control for a Tiltrotor," 80th Annual Vertical Flight Society Forum, 2024, pp. 1–20. https://doi.org/10.4050/F-0080-2024-1348
5. Lim, S. K. Y., Boon, Z. Y., and Wang, J., "Trajectory Modelling of Transition Regime Using Blade Element Method for Different EVTOL Aircraft Configurations," 49th European Rotorcraft Forum, 2023.
6. Pradeep, P., and Wei, P., "Energy Optimal Speed Profile for Arrival of Tandem Tilt-Wing EVTOL Aircraft with RTA Constraint," 2018 IEEE CSAA Guidance, Navigation and Control Conference, 2018, pp. 1–6. https://doi.org/10.1109/GNCC42960.2018.9018748
7. Chauhan, S. S., and Martins, J. R. R. A., "Tilt-Wing EVTOL Takeoff Trajectory Optimization," Journal of Aircraft, Vol. 57, No. 1, 2020, pp. 93–112. https://doi.org/10.2514/1.C035476
8. Panish, L., and Bacic, M., "Transition Trajectory Optimization for a Tiltwing VTOL Aircraft with Leading-Edge Fluid Injection Active Flow Control," AIAA SciTech 2022 Forum, 2022. https://doi.org/10.2514/6.2022-1082
9. Kang, N., Lu, L., and Whidborne, J., "Energy Optimization Strategies for Automatic Tiltrotor Electric Vertical Takeoff and Landing Aircraft," Journal of Guidance, Control, and Dynamics, Vol. 48, No. 5, 2025, pp. 1196–1200. https://doi.org/10.2514/1.G008466
10. Di Vito, V., Dziugiel, B., Melo, S., Ten Thije, J. T., Duca, G., Liberacki, A., Hesselink, H., Giannuzzi, M., Menichino, A., Montaquila, R. V., Cerasuolo, G., and Witkowska Konieczny, A., "Integrating Urban Air Mobility into Smart Cities: A Proposal for Relevant Use Cases in the next Decades," Aircraft Engineering and Aerospace Technology, Vol. 97, No. 1, 2025, pp. 2–12. https://doi.org/10.1108/AEAT-03-2024-0081
11. Feary, M. S., Kaneshige, J., Lombaerts, T., Shish, K., and Haworth, L., "Evaluation of Novel EVTOL Aircraft Automation Concepts," AIAA Aviation 2023 Forum, 2023.
12. Perfect, P., Jump, M., and White, M. D., "Handling Qualities Requirements for Future Personal Aerial Vehicles," Journal of Guidance, Control, and Dynamics, Vol. 38, No. 12, 2015, pp. 2386–2398. https://doi.org/10.2514/1.G001073
13. Perfect, P., Jump, M., and White, M. D., "Methods to Assess the Handling Qualities Requirements for Personal Aerial Vehicles," Journal of Guidance, Control, and Dynamics, Vol. 38, No. 11, 2015, pp. 2161–2172. https://doi.org/10.2514/1.G000862

14. Bardusch, R. E., Deal, P. L., Jaquet, B. M., and Riley, D. R., “A Study of Gemini Agena Docking Using a Fixed Base Simulator Employing a Closed Circuit Television System,” NASA-TN-D-3112, 1965.

15. Bachelder, E., and Aponso, B., “Novel Methods for Estimating Bandwidth and Stability Margins of Pilot-in-Loop Systems,” 45th European Rotorcraft Forum, 2019.

16. Lu, L., Jump, M., White, M., and Perfect, P., “Development of Occupant-Preferred Landing Profiles for Personal Aerial Vehicles,” Journal of Guidance, Control, and Dynamics, Vol. 39, No. 8, 2016, pp. 1805–1819. https://doi.org/10.2514/1.G001608

17. Li, W.C., Horn, A., Sun, Z., Zhang, J., and Braithwaite, G., “Augmented Visualization Cues on Primary Flight Display Facilitating Pilot’s Monitoring Performance,” International Journal of Human-Computer Studies, Vol. 135, 2020, p. 102377. https://doi.org/10.1016/j.ijhcs.2019.102377

18. Hart, S. G., and Staveland, L. E., “Development of NASA-TLX (Task Load Index): Results of Empirical and Theoretical Research,” Advances in Psychology, Vol. 52, 1988, pp. 139–183.

19. Drela, M., and Youngren, H., “Athena Vortex Lattice Version 3.36,” MIT, Cambridge, 2017.

20. Drela, M., “QPROP Version 1.22,” Cambridge, 2007.

21. Chappell, D., “In-Plane Forces and Moments on Installed Inclined Propellers at Low Forward Speeds,” ESDU 89047 Amendment E, 2021.

22. Morelli, E. A., and Klein, V., “Aircraft System Identification: Theory and Practice,” Sunflyte Enterprises, Williamsburg, 2016.

23. Maré, J. C., “Aerospace Actuators 2: Signal-by-Wire and Power-by-Wire,” John Wiley, Hoboken, 2017.

24. Padfield, G. D., “Helicopter Flight Dynamics: Including a Treatment of Tiltrotor Aircraft,” John Wiley & Sons, Chichester, 2018.

25. Duda, H., “Prediction of Pilot-in-the-Loop Oscillations Due to Rate Saturation,” Journal of Guidance, Control, and Dynamics, Vol. 20, No. 3, 1997, pp. 581–587. https://doi.org/10.2514/2.4080

26. Kang, N., Lu, L., and Whidborne, J., “Minimum Energy Automatic Flight Control Design for EVTOL Transition Phases,” 81st Annual Vertical Flight Society Forum, 2025.

27. Hess, R. A., “Modeling the Pilot Detection of Time-Varying Aircraft Dynamics,” Journal of Aircraft, Vol. 49, No. 6, 2012, pp. 2100–2104. https://doi.org/10.2514/1.C031805

28. Korek, W. T., Beecroft, P., Lone, M., Bragado Aldana, E., Mendez, A., Enconniere, J., Asad, H. U., Grzedzinski, K., Milidere, M., Whidborne, J., Li, W.C., Lu, L., Alam, M., Asmayawati, S., Del Barrio Conde, L., Hargreaves, D., and Jenkins, D., “Simulation Framework and Development of the Future Systems Simulator,” The Aeronautical Journal, Vol. 128, No. 1330, 2024, pp. 2754–2780. https://doi.org/10.1017/aer.2024.91

29. Dollinger, D., Fricke, T., and Holzapfel, F., “Control Inceptor Design for Remote Control of a Transition UAV,” AIAA Aviation Forum, 2019. https://doi.org/10.2514/6.2019-3268

30. Dollinger, D., Reiss, P., Angelov, J., Löbl, D., and Holzapfel, F., “Control Inceptor Design for Onboard Piloted Transition VTOL Aircraft Considering Simplified Vehicle Operation,” AIAA Scitech 2021 Forum, 2021. https://doi.org/10.2514/6.2021-1896

31. Lombaerts, T., Kaneshige, J., and Feary, M., “Control Concepts for Simplified Vehicle Operations of a Quadrotor EVTOL Vehicle,” AIAA Aviation 2020 Forum, 2020. https://doi.org/10.2514/6.2020-3189

32. Feary, M., Kaneshige, J., Lombaerts, T., Haworth, L., Archdeacon, J., Iwai, N., Shish, K., Deshmukh, R., Torron, I., and Hardy, G., “Evaluation of Novel V/STOL Aircraft Pilot Interface Concepts — Version 1.15,” DOT/FAA/TC-24/6, 2024.

33. Feroskhan, M., Lu, X., Wang, J., Lee, E., and Khoo, G., “Comparing Different Pilot Control Schemes for EVTOL and Powered-Lift Aircraft,” Vertical Flight Society 81st Annual Forum, 2025, pp. 1–24. https://doi.org/10.4050/F-0081-2025-171

34. Pupil Labs, “Pupil Neon Technical Specifications,” 2025. Retrieved 26 June 2025. https://pupil-labs.com/products/neon/specs

35. Ford, C. C., Bugmann, G., and Culverhouse, P., "Modeling the Human Blink: A Computational Model for Use Within Human-Robot Interaction," International Journal of Humanoid Robotics, Vol. 10, No. 01, 2013, p. 1350006.

APPENDIX A

NASA Task Load Index

Hart and Staveland's NASA Task Load Index (TLX) method assesses work load on five 7-point scales. Increments of high, medium and low estimates for each point result in 21 gradations on the scales.

Name	Task	Date

Mental Demand — How mentally demanding was the task?

Very Low — Very High

Physical Demand — How physically demanding was the task?

Very Low — Very High

Temporal Demand — How hurried or rushed was the pace of the task?

Very Low — Very High

Performance — How successful were you in accomplishing what you were asked to do?

Perfect — Failure

Effort — How hard did you have to work to accomplish your level of performance?

Very Low — Very High

Frustration — How insecure, discouraged, irritated, stressed, and annoyed wereyou?

Very Low — Very High

Figure A NASA TLX Questionnaire.

APPENDIX B

1	I felt I was in control of the events.	
	0	100
	Strongly Disagree	Strongly Agree
2	I experienced discomfort with the task.	
	0	100
	Strongly Disagree	Strongly Agree
3	The movement in the virtual environment seemed unnatural.	
	0	100
	Strongly Disagree	Strongly Agree
4	I felt engaged in the virtual reality environment.	
	0	100
	Strongly Disagree	Strongly Agree
5	The interaction with the guidance seems natural.	
	0	100
	Strongly Disagree	Strongly Agree

Figure B Comfort Rating Scale for Piloted Simulation Study.

APPENDIX C

Table C FTM and its performance criteria for Conversion/re-conversion

TITLE	**Conversion/re-conversion FTM – level flight**		
Mission; Flight Mode	Hover mode, conversion/re-conversion mode, aircraft mode		
Critical HQs	Check stability, agility and comfort rating during minimum energy conversion and re-conversion rotor tilting profiles.		
Objectives	Check ability to perform level flight accelerations and decelerations via rotor tilting, while maintaining height and heading.		
Manoeuvre Description	**Conversion:** • Start a stabilised hover at 100 ft height. In the GVE, initiate a longitudinal acceleration to a cruise airspeed of 105 kts, and maintain altitude constant with pitch attitude during conversion. Upon reaching the target airspeed, initiate a deceleration by holding altitude constant with pitch attitude. **Re-conversion:** • Start a trimmed flight at a cruise airspeed of 105 kts and 100 ft height. In the GVE, initiate a longitudinal deceleration to a stabilised hover, and maintain altitude constant with pitch attitude during reconversion. Upon reaching the hover speed, initiate a deceleration by holding altitude constant with pitch attitude.		
Performance Standards		**Desired**	**Adequate**
	• Complete conversion within time $T < \Delta T + T_{\min}$	$T_{\min} = 32$ sec $\Delta T = 8$ sec	$T_{\min} = 32$ sec $\Delta T = 15$ sec
	• Complete re-conversion within time $T < \Delta T + T_{\min}$	$T_{\min} = 69$ sec $\Delta T = 10$ sec	$T_{min} = 69$ sec $\Delta T = 20$ sec
	• Terminal airspeed to be captured within X kts:	$\pm$ 2 kts	$\pm$ 3 kts
	• Maintain acceleration within X g of wing-level mode:	$\pm$ 0.3 g	$\pm$ 0.6 g
	• Maintain pitch within X deg of wing-level mode:	$\pm$ 5 deg	$\pm$ 10 deg
	• Maintain heading within X deg of initial heading:	$\pm$ 5 deg	$\pm$ 10 deg
	• Maintain altitude within X feet of initial height:	$\pm$ 15 ft	$\pm$ 30 ft
	• Maintain lateral track within X feet of initial position:	$\pm$ 0.3 D	$\pm$ 0.6 D
	• Any oscillations or inter-axis coupling shall not be:	Undesirable	Objectionable
	• Control harmony between axes shall not be:	Undesirable	Objectionable